Controlled Defects in Semiconducting Carbon Nanotubes Promote Efficient Generation and Luminescence of Trions

Alexandra H. Brozena,[†] Jarrett D. Leeds,[†] Yin Zhang,[†] John T. Fourkas,[†,‡,§,∥] and YuHuang Wang[†,§,*]

[†]Department of Chemistry and Biochemistry, [‡]Institute for Physical Science and Technology, [§]Maryland NanoCenter, and [∥]Center for Nanophysics and Applied Materials, University of Maryland, College Park, Maryland 20742, United States

ABSTRACT We demonstrate efficient creation of defect-bound trions through chemical doping of controlled sp^3 defect sites in semiconducting, single-walled carbon nanotubes. These tricarrier quasi-particles luminesce almost as brightly as their parent excitons, indicating a remarkably efficient conversion of excitons into trions. Substantial populations of trions can be generated at low excitation intensities, even months after a sample has been prepared. Photoluminescence spectroscopy reveals a trion binding energy as high as 262 meV, which is substantially larger than any previously reported values. This discovery may have important ramifications not only for studying the basic physics of trions but also for the application of these species in fields such as photonics, electronics, and bioimaging.

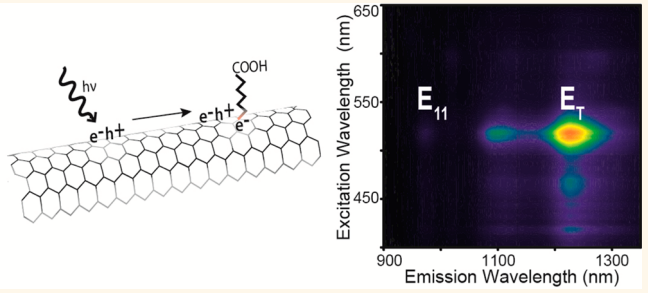

KEYWORDS: carbon nanomaterials · photophysics · defects · chemical functionalization · exciton · spectroscopy

A trion is a charged, quasi-particle composed of two electrons and one hole (or *vice versa*). The existence of this H^- (or H_2^+) analogue was first predicted by Lampert in 1958,[1] but decades would pass before this tricarrier species would be observed experimentally, first in quantum wells,[2,3] then in quantum dots,[4] and more recently in single-walled carbon nanotubes (SWCNTs).[5−9] Observation of SWCNT trions has been made possible *via* chemical or electrochemical doping techniques[5,6] and by multiexciton generation using high-power lasers.[7,9] These experimental conditions promote excess charge carriers, which are required for the creation of the tricarrier species upon photoexcitation. Both experiments and theory have demonstrated that SWCNT trion emission is dependent on nanotube structure and red-shifted from the E_{11} exciton photoluminescence further into the near-IR.[5−7,10,11] Unlike the situation for bulk semiconductors, in SWCNTs, differentiation between trion and exciton photoluminescence is made possible by strong Coulomb interactions.[12] These interactions increase the trion binding energy (the energy required to strip the extra carrier from the exciton),[13] resulting in a new peak that is red-shifted from the exciton emission in the photoluminescence spectrum.

Trions are interesting from both fundamental and technological perspectives. With an extra charge and nonzero spin, the trion provides opportunities to manipulate spin[14] and to control the optical properties of semiconducting nanomaterials.[15] However, with just a 1−20 meV binding energy,[4,16] trions in semiconductor quantum wells and quantum dots are unstable except at cryogenic temperatures. SWCNT trions show a markedly higher binding energy, with values as large as 215 meV having been reported.[5,7] This increased binding energy enables SWCNT trions to be observed even at room temperature. However, in the few previous cases in which SWCNT trions have been observed, they have been present only as a minority carrier.[5−9]

Here, we demonstrate that trions can be efficiently generated as bound quasi-particles

* Address correspondence to yhw@umd.edu.

Received for review September 22, 2013 and accepted March 26, 2014.

Published online March 26, 2014
10.1021/nn500894p

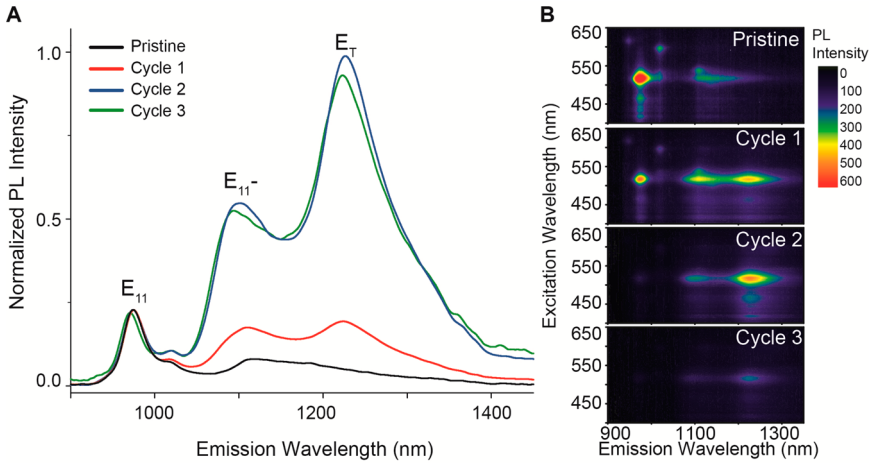

Figure 1. Trion photoluminescence is observed in covalently functionalized SWCNTs. (A) Sidewall propagative alkylcarboxylation of (6,5) SWCNTs induces two new photoluminescence peaks, E_{11}^- and E_T. To highlight the changing ratio of E_{11}^- and E_T with increased functionalization degree/reaction cycles, the photoluminescence peaks were normalized by the E_{11} intensity. (B) Excitation–emission maps of the functionalized samples scaled by the absorbance at 570 nm (the E_{22} transition).

under aqueous conditions in covalently functionalized, semiconducting SWCNTs, despite the fact that covalent defects tend to quench photoluminescence of the parent excitons from which trions may form.[17] The improved efficiency observed here is due to defect-promoted trapping of charges and excitons. Covalent sp^3 defects have been shown to split the frontier orbitals of a SWCNT, creating localized potential wells within the extended sp^2 carbon network.[18,19] Each sp^3 center is valence-satisfied and does not donate an electron. This situation is distinctly different from that of an atomic dopant in a semiconductor; in the latter case, excitation leads to creation of donor-bound excitons, in which the donor electron is strongly correlated to the dopant.[2] We demonstrate that these controllably added defect wells stabilize not only the excess electrons or holes added in SWCNTs but also the photogenerated excitons. Trapping the exciton and extra charge carrier at the same defect site enables a bound trion to form efficiently.

To introduce sp^3 defects, SWCNTs are covalently functionalized by two methods: (1) Billups–Birch propagative sidewall alkylcarboxylation chemistry using sodium-charged liquid ammonia[19,20] and (2) oleum-based diazonium chemistry (100% H_2SO_4, 20% free SO_3).[21] Following either type of functionalization, trion photoluminescence is observed in the emission spectrum of individually dispersed (6,5) SWCNTs as a new peak that is substantially red-shifted from the E_{11} exciton. The energy shift gives a trion binding energy of ~262 meV, which is approximately 70 meV more than the highest trion binding energy reported previously for (6,5) SWCNTs.[7] The strong dependence of the magnitude of this new feature on both covalent functionalization and doping conditions is also distinct from previous observations of trions in SWCNTs. Because this new emission is observed for covalent chemistries that have opposite doping effects on local electronic structure, we propose that trion emission is a universal behavior for covalently functionalized SWCNTs that have been doped with electrons or holes. This trion feature provides crucial insight into the relationship between SWCNT doping and surface defect character, which is particularly important as SWCNTs are of interest for semiconductor applications in which doping is a fundamental property of device behavior.[22]

RESULTS AND DISCUSSION

The SWCNTs were functionalized with hexanoic acid groups *via* the Billups–Birch reaction[20] and were individually dispersed in D_2O with 1 wt % sodium dodecylbenzenesulfonate (SDBS). Excitation of the (6,5) E_{22} transition (570 nm) reveals new emission features at 1092 and 1225 nm (Figure 1). These peaks are labeled E_{11}^- and E_T and have red shifts of 136 and 262 meV from the (6,5) E_{11} exciton transition (973 nm), respectively. The weak emission features between 1100 and 1200 nm arise from (8,4) and (9,2) SWCNT chiralities present in the starting material.[23] Excitation wavelength studies rule out these impurities as the cause of the E_{11}^- and E_T peaks (Supporting Information Figure S1). As the functionalization degree increases with each alkylcarboxylation cycle,[20] the absolute E_{11} photoluminescence intensity becomes progressively weaker due to decreased SWCNT absorption.[19] The relative intensities of the E_{11}^- and E_T peaks are maximized after two reaction cycles. The absolute photoluminescence intensity indicates that after two reaction cycles E_T has approximately one-half the intensity of the pristine sample E_{11} peak (Figure 1B).

Photoluminescence excitation spectra reveal that the covalent-defect-activated E_{11}^- and E_T photoluminescence peaks are generated upon irradiation at the

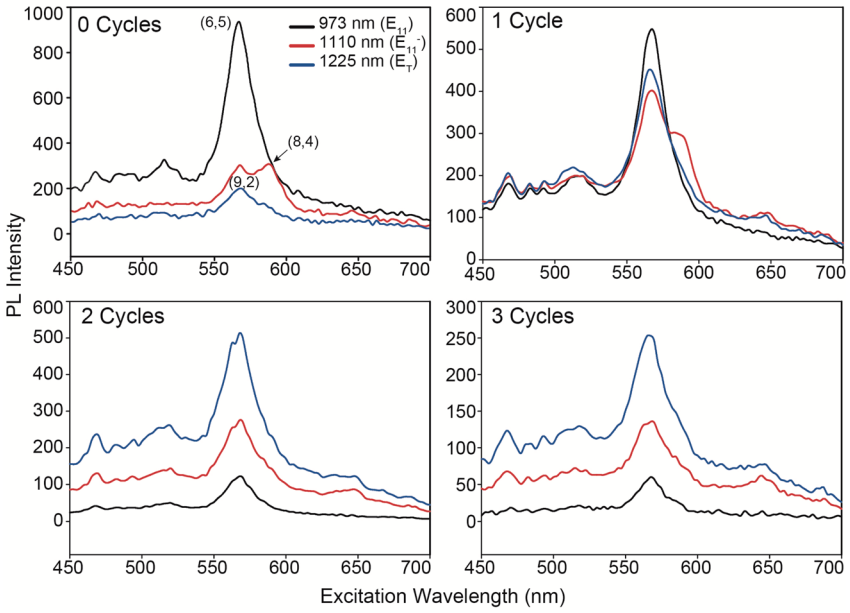

Figure 2. Photoluminescence excitation spectra of (6,5) SWCNTs before functionalization and after up to three cycles of functionalization by the Billups–Birch reaction. Photoluminescence is monitored at 973, 1110, and 1225 nm (E_{11}, E_{11}^-, and E_T, respectively). After covalent functionalization, the E_{11}^- and E_T peaks appear upon excitation at the wavelength of the (6,5) E_{22} transition (570 nm). Broad features corresponding to (8,4) and (9,2) species are visible in the zero-cycle and one-cycle spectra. Increasing covalent functionalization largely removes the optical signatures of these lower-concentration species, as is also reflected in the decreased intensity of the (6,5) E_{11} emission.

(6,5) E_{22} excitation wavelength of 570 nm (Figure 2). These new peaks also appear upon irradiation with the (6,5) E_{11} excitation wavelength for this chirality (970 nm) (Supporting Information Figure S2). Together, these observations indicate that the E_{11}^- and E_T peaks arise from (6,5) SWCNTs.

A previous study of this same reaction by Zhang *et al.*[19] using Raman spectroscopy revealed that the reaction produces covalent defects on the nanotube sidewalls. Density functional theory calculations demonstrated that the introduction of sp^3 defects into the sp^2 carbon lattice splits the E_{11} exciton transition. This splitting results in an optically active, lower-energy transition that is red-shifted from E_{11} (*i.e.*, the E_{11}^- peak in the photoluminescence spectra).[18,19] These new photoluminescence features do not appear in the absorption spectrum of the functionalized SWCNTs (Supporting Information Figure S3). By applying the same chemistry to HiPco and (7,6)-enriched CoMoCat SWCNT samples, the position of E_T was determined for additional nanotube chiralities by using excitation–emission photoluminescence maps. The energy shift of E_T from the E_{11} emission correlates inversely with SWCNT diameter and suggests $2n + m$ family branching behavior (Figure 3). A more complete chiral spread to confirm this branching pattern could not be performed due to superimposed chiral features in the photoluminescence excitation–emission spectra.

In the Billups–Birch reaction, SWCNTs are reduced using sodium in liquid ammonia. Reduction electrostatically disperses the nanotubes and generates alkyl radicals for covalent functionalization by electron transfer from the reduced nanotubes. This reaction could also n-dope the SWCNTs. Such doping would be conducive to the formation of trions.[6] To test whether E_T arises from trion photoluminescence, Billups–Birch-functionalized SWCNTs were dispersed in oleum to counteract potential n-doping effects. The sample was washed copiously with water to remove excess protons arising from the superacid treatment and then was dispersed in D_2O with 1 wt % SDBS for spectroscopic studies.

Excitation–emission maps of samples treated in this manner reveal a striking decrease in the intensity of the E_T peak (Figure 4A,B) that is also visible in the emission spectrum (Supporting Information Figure S4). The retention of the defect-activated E_{11}^- peak indicates that the nanotubes are still functionalized after superacid treatment, although E_{11}^- is red-shifted by 45 nm relative to its position in the sample that was not treated with oleum (Supporting Information Figure S5). The increase in the E_{11} emission intensity after dispersion of the SWCNTs in oleum is consistent with a decreased doping concentration. SWCNT photoluminescence is well-known to be highly sensitive to the presence of dopants.[6,24] Additionally, the absorption spectrum regains optical density in the E_{11} and E_{22} peaks after dispersion in oleum (Supporting Information Figure S6), which implies that dispersing the previously sodium-reduced SWCNTs in superacid decreases the dopant concentration. The use of highly reducing conditions to generate the E_T

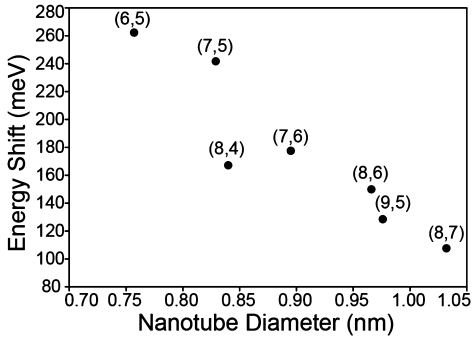

Figure 3. Inverse diameter dependence of the energy shift of E_T from the E_{11} emission is consistent with previous reports of SWCNT trion photoluminescence, including some indication of branching $2n + m$ family behavior as seen for the (8,4) and (7,6) chiralities. The energy shifts were extracted from previously published[19] excitation−emission maps of Billups−Birch reaction-functionalized HiPco and purified CoMoCat (7,6) samples.

photoluminescence peak is consistent with the results of recent SWCNT trion studies, in which optical or electrochemical doping of excess charge carriers in suspended SWCNTs generated trion photoluminescence.[5−7] The change we observe in the intensity of E_T after oleum dispersion strongly suggests that this photoluminescence is related to doping, which in addition to the chirality/diameter dependence of E_T supports the assignment of this new peak as trion emission.[5−7]

Localized doping of electrons or holes at covalent functional sites could also explain the observed red shift of the defect-induced E_{11}^- peak after oleum treatment (Figure 4B). The splitting degree of the E_{11} frontier orbitals as a result of sp^3 carbon atoms within the SWCNT sp^2 lattice should decrease with distance from the defect site,[19,25] creating a distribution of energy levels that can be filled by reductive chemical doping. This distribution is consistent with the large spatial extent (nearly 2 nm) of a defect on a highly ordered pyrolytic graphite, as resolved by Kelly *et al.* using scanning tunneling microscopy.[26] Dispersing these functionalized SWCNTs in oleum depletes the n-doped energy levels around the defect site, effectively lowering the transition energy and resulting in the red shift of the E_{11}^- peak after superacid treatment.

To test this defect hypothesis, unfunctionalized SWCNTs were dispersed in either oleum or sodium and liquid ammonia. No new photoluminescence peaks appeared after this treatment (Figure 4C). These controls indicate that defects are necessary for the successful reduction or oxidation of the nanotubes under these doping conditions. Simultaneous reduction and functionalization of the SWCNTs causes the trion peak to appear (Figure 1). However, when SWCNTs are reduced (or oxidized) without the addition of functional groups, the E_T peak is not present. This observation suggests that to dope the nanotubes effectively, defects must either be added during the reduction or be present previously.

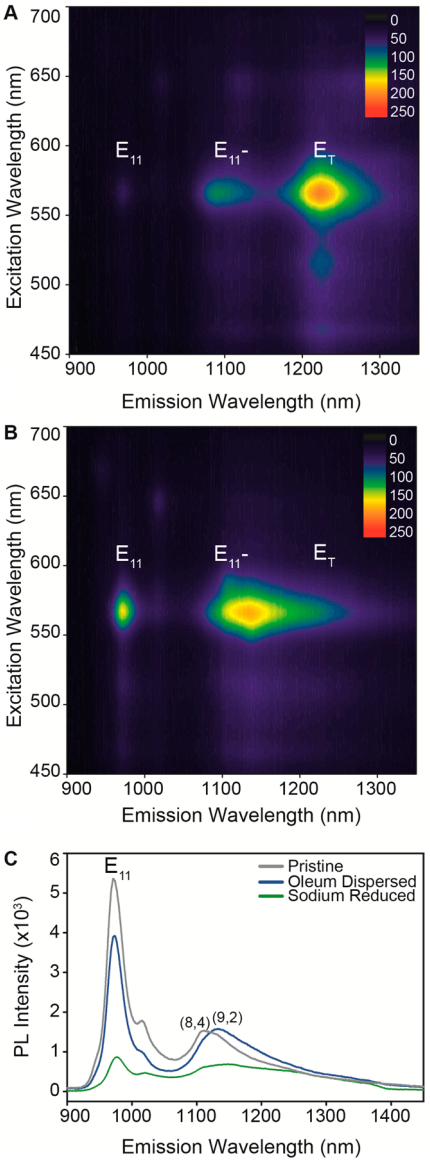

Figure 4. Emission spectra of functionalized and pristine SWCNTs under different doping conditions. SDBS-D_2O (1 wt %) suspended, three-cycle, Billups−Birch-alkylcarboxylated SWCNTs (A) before and (B) after superacid treatment. The intensity of E_T and the associated phonon-assisted sidebands diminishes after reducing conditions are diminished. (C) Dispersion of pristine SWCNTs (gray) in oleum (blue) or with sodium in liquid ammonia (green), without functionalization, fails to produce E_T in the photoluminescence spectra (570 nm excitation). The broad peak between 1100 and 1200 nm is due to (8,4) and (9,2) species also present in solution.

Since oleum neutralizes the effects of n-doping-generated trion photoluminescence, we investigated whether positive trions could be generated using oleum-based covalent chemistry. (6,5)-enriched CoMoCat SWCNTs were functionalized with 4-nitrobenzene groups using an *in situ* diazonium reaction in oleum.[21] As with the alkylcarboxylated SWCNTs, two new peaks appear in the excitation/emission maps after functionalization with this superacid chemistry, although E_T is observed to be broader for this functionalization

chemistry compared to the hexanoic-acid-functionalized samples (Supporting Information Figure S7). These new peaks have energy shifts of 174 meV (E_{11}^-) and approximately 262−278 meV (E_T) relative to the (6,5) E_{11} emission at 970 nm. The shift in the position of E_{11}^- compared to the hexanoic-acid-functionalized SWCNTs created by Billups−Birch reduction is likely due to the difference in the electron-withdrawing capacity of the functional groups.[18,19] An excitation study of the functionalized SWCNTs clearly indicates that the E_{11}^- and E_T features appear following excitation at the same wavelength as the (6,5) species and do not arise from chiral impurities, which are excited at different wavelengths (Supporting Information Figure S8). Raman spectroscopy of the 4-nitrobenzene-functionalized SWCNT sample shows an increase in the ratio of the intensity of the D band (~1300 cm^{-1}, sp^3-hybridized carbons atoms) to the G band (~1580 cm^{-1}, sp^2-hybridized) as compared to the nonfunctionalized SWCNT starting material. This observation indicates that covalent functionalization occurs on the nanotube sidewalls after SWCNTs are subjected to this superacid chemistry (Supporting Information Figure S9).

In the diazonium chemistry used, oleum disperses SWCNTs for functionalization by protonating the weakly basic nanotubes and enabling intercalation of the sulfate ion, electrostatically exfoliating the nanotube bundles in solution. It is possible that this process also p-dopes the SWCNTs. To test whether the E_T peak has any relation to the SWCNT oxidative state, we reduced the oven-dried, functionalized sample with sodium in liquid ammonia. After reduction, the sample was redispersed with 1 wt % SDBS-D_2O for spectral analysis.

As expected, SWCNT doping diminishes the photoluminescence intensity (Supporting Information Figure S10), but the relative ratio of the E_{11} and E_{11}^- peak intensities remains fairly stable (Figure 5A). Consistent with this observation, the Raman spectra of these reduced samples change little compared to the functionalized-alone material, suggesting a constant degree of functionalization (Supporting Information Figure S11). Adding 0.75 equiv of sodium relative to the number of moles of carbon atoms that make up the functionalized SWCNT sample results in a substantial drop in the intensity of the E_T peak relative to that of the E_{11}^- peak (Figure 5A). However, treatment with 1.5 equiv of sodium leads to an increase in the intensity of E_T relative to E_{11}^-. These results indicate that the intensity of the E_T peak is related to the oxidative state of the SWCNTs. If we assume that the 4-nitrobenzene-functionalized SWCNTs are p-doped after functionalization in oleum, then the addition of 0.75 equiv of sodium would effectively reduce the nanotubes. However, after treatment with double that amount of sodium, E_T increases, suggesting that the 1.5 equiv of sodium reduces the SWCNTs to an extent that exceeds

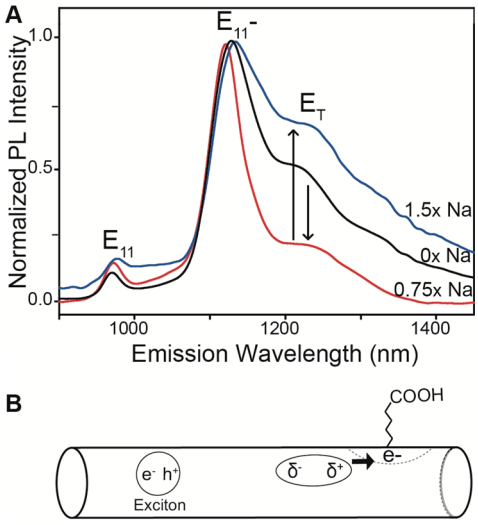

Figure 5. Chemical modulation of trion photoluminescence in the 4-nitrobenzene-functionalized SWCNTs through electron doping with different numbers of equivalents of sodium. (A) Spectra are normalized to the E_{11}^- peak, as the intensity of E_{11} changes dramatically after doping concentrations are modified, but the ratio of E_{11}^- to E_{11} remains almost constant due to the unchanging functional degree of the sample. Sodium equivalents are calculated relative to the number of moles of carbon atoms that make up the functionalized SWCNT sample. (B) Schematic depiction of the mechanism of enhanced trapping of excitons at charged defect sites. The symmetric exciton wave function will become polarized in the vicinity of a charged defect, resulting in rapid trapping of the exciton.

the initial hole dopant concentration. This process leaves the SWCNTs in a reduced state as opposed to an oxidized state. The resultant increase in the E_T intensity suggests that this peak serves as an indicator of the dopant concentration of either positive or negative charges. It is difficult to know the exact concentration of SWCNT dopants under these conditions (and there is probably sidewall protonation that reacts with the added sodium, as well); quantification of the dopant concentration will require better-controlled titration experiments.

These changes in the intensity of E_T as a function of doping are also reflected in the peak shift and width changes of E_{11}^- (Supporting Information Figure S12). Before sodium reduction, the E_{11}^- peak of the 4-nitrobenzene-functionalized sample appears at 1126 nm and has a full width at half-maximum (fwhm) of 43 meV. After reduction by 0.75 equiv of sodium, the E_{11}^- fwhm decreases to 37 meV and the peak is blue-shifted slightly to 1124 nm. SWCNT optical spectra are highly sensitive to dopants, demonstrating significant peak intensity loss and broadening with increasing dopant concentration.[24] The decrease in the fwhm of E_{11}^- after reduction suggests that the injected electrons induce at least partial cancellation of the hole dopants created during the original oleum synthesis. The spatial dependence of defect-activated E_{11} splitting[25] may create an isolated "band-like" electronic structure

that could also contribute to the observed narrowing of E_{11}^- upon dopant removal. This depletion of hole dopants by the addition of 0.75 equiv of sodium also causes a corresponding decrease in the E_T emission intensity. While 0.75 equiv of added sodium is likely to be far in excess to the actual number of implanted, p-doped sp^3 defects (<5% of total carbon atoms),[20] protons that remain physisorbed to the nanotube sidewalls (after functionalization in oleum and processing in water) can effectively cancel out the effects of the excess sodium due to the metal/acid reaction.

The addition of 1.5 equiv of sodium red-shifts the E_{11}^- peak to 1127 nm and increases its fwhm to 44 meV, which indicates that the dopant concentration is increased compared to the 0.75 equiv of sodium addition. This observation is also consistent with 1.5 equiv of Na bringing the sample to the n-doped regime. The reduction and oxidation of the 4-nitrobenzene-functionalized SWCNTs demonstrates both positive and negative trion photoluminescence at nearly identical positions (~1225 nm). The previous observation of *in situ* generated positive and negative trions at nearly the same energy shift was explained by the small effective mass difference between holes and electrons.[6] If there is in fact a difference in positive and negative trion shifts here, it is difficult to resolve due to the background emission of other chiralities present within the sample.

How can the changes in the relative photoluminescence intensities of the three peaks with the addition of sodium be explained? Although the intensity of E_T changes with the dopant concentration in Figure 5, the relative intensity of E_{11}^- remains fairly stable (as shown by the nearly constant ratio with E_{11}), even though the total number of traps (doped plus undoped) cannot change. We propose that this phenomenon arises from a difference between the trapping times at charged (doped) and noncharged (neutral) defects. An exciton's wave function is symmetric;[27,28] however, diffusion to a charged defect site may cause polarization of the quasi-particle. Analogous to hydrogen atoms,[29] the polarizability, α, of an exciton is given by

$$\alpha = \frac{9}{2}\left(\frac{4\pi\varepsilon_0\hbar^2 m_e}{e^2}\right)^3 \frac{1}{\mu^3} \qquad (1)$$

where ε_0 is the permittivity of free space, $\hbar$ is the reduced Planck's constant, e is elementary charge, $\mu = (m_e m_h)/(m_e + m_h)$ m_e is the electron mass, and m_h is the hole mass. Since there is little difference in mass for holes and electrons in carbon nanotubes,[6] the nanotube exciton has a smaller reduced mass than that of hydrogen atom. Furthermore, the effective mass for electrons in a (6,5) SWCNT is approximately 70% of the rest mass.[30] As a result, the polarizability of nanotube excitons is a factor of approximately 22 times larger than that of hydrogen (*i.e.*, the exciton polarizability is three times as polarizable as an iodine atom).[31] The high polarizability of excitons is expected to result in enhanced attraction of the exciton to charged sites, leading to a higher exciton mobility (and therefore more rapid trapping) in the vicinity of charged defects as compared to neutral defects (Figure 5B). Time-resolved photoluminescence and transient absorption experiments could shed additional light on these processes.

In both the negative and positive trion generation chemistries, E_T does not appear in the absence of defects (Supporting Information Table S1). For a better understanding of the defect dependence of E_T, we used an alternative chemistry to generate SWCNT defects under conditions that were neither highly reductive nor highly oxidative. These experiments allow us to separate the effects of functionalization and reduction/oxidation on the photoluminescence spectra, which cannot be achieved using the oleum-based diazonium and the Billups–Birch reduction chemistries.

Oleum-free, aqueous-phase, diazonium-based chemistry was chosen for its ability to add defects controllably to SWCNTs by varying the reactant concentration and reaction time. After functionalizing SWCNTs with freshly synthesized 4-nitrobenzene diazonium salt dispersed in D_2O with 1 wt % sodium dodecylsulfonate (SDS), the E_{11}^- peak is observed as expected (Figure 6A).[18]

The diazonium-functionalized SWCNTs were then reduced using the same conditions as with the Billups–Birch alkylation, but without the addition of new functional groups. Although the E_T peak does not appear when pristine nanotubes are reduced by solvated electrons, it is present upon reduction of diazonium-functionalized SWCNTs (Figure 6B). This observation verifies that trion emission from reduced SWCNTs is defect-dependent.

The trion binding energy (~260 meV, derived from the energy shift for E_T) is significantly larger than was observed in previous SWCNT trion studies, in which a binding energy of ~170–190 meV was reported for the (6,5) nanotube chirality.[5−7] We hypothesize that trapping of trions at the chemically implanted defect sites leads to a greater binding energy. Covalent functionalization splits the E_{11} state, which can then trap excitons at a lower energy level,[19] resulting in red-shifted E_{11}^- emission and, correspondingly, a larger binding energy for the bound trions. Trapping should shift the trion binding energy by approximately the same amount as the exciton energy, as long as the trion binding energy does not change significantly at the defect. Thus, we would expect that emission from defect-bound trions should be red-shifted by approximately the defect-activated well depth as compared to emission from nontrapped trions (Scheme 1C). Determining the well depth corresponding to these defects

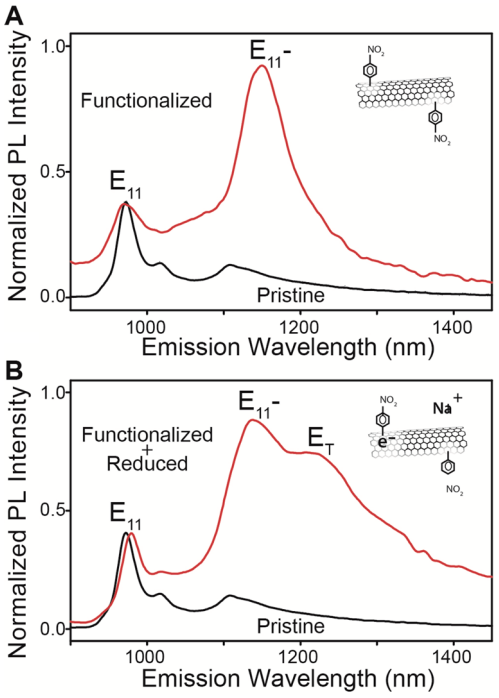

Figure 6. Defect-dependent reduction of 4-nitrobenzene-functionalized SWCNTs. (A) Covalent functionalization of SWCNTs by 4-nitrobenzene under neutral, aqueous conditions produces the E_{11}^- peak but not the E_T peak. (B) Subsequent charging by sodium of the functionalized SWCNTs generates the E_T peak, suggesting a defect dependence of trion emission under these conditions.

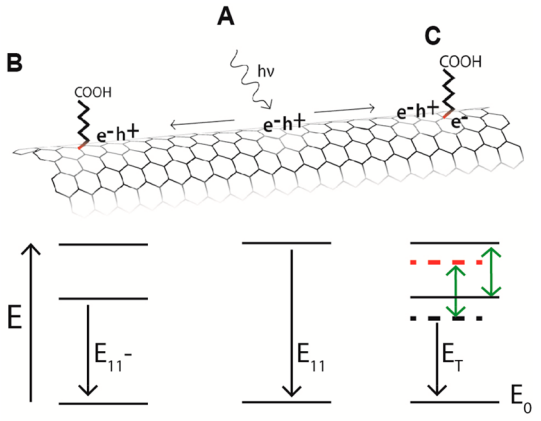

Scheme 1. Proposed exciton decay pathways in a functionalized carbon nanotube under n-doping conditions. Energy-level diagrams for (A) the nonfunctionalized, (B) undoped, and (c) doped defect sites. Ground-state energy levels are not absolute and are pictured to illustrate the relative energy differences among the excited states. The observed emission peaks arise from the E_{11}, defect-activated E_{11}^-, and E_T trion states. The dashed lines in the doped energy level diagram (C) correspond to the trion energy at nonperturbed (red) and defect sites (black), in which the defect-generated trion energy level is depressed by approximately the same amount as the energy difference between E_{11} and E_{11}^- (green double arrows).

should reveal whether this hypothesis is consistent with the observed increased trion energy shift.

Photoluminescence of the three-cycle alkylcarboxylated SWCNT sample was monitored as temperature was ramped up and down between 10 and 90 °C. Changes in the ratio of the E_{11} integrated peak area to the E_{11}^- integrated peak area at different temperatures allow us to deduce the difference in energy between these two levels, that is, the effective depth of the defect wells.[18,19,25] A van't Hoff plot based on the temperature-dependent ratio of the E_{11} peak area to the E_{11}^- peak area yields a potential well depth of 75.3 ± 4.6 meV for the implanted defects (Supporting Information Figure S13). The additional ~75 meV stabilization of the ~180 meV (6,5) SWCNT trion energy shift[5−7] is in good agreement with our observed 262 meV energy shift and is consistent with theoretical calculations that suggest that trion binding energies are greater at defect sites in quantum-confined systems.[32]

From these results, it appears that the combination of covalent functionalization and doping of SWCNTs creates three different radiative pathways for an exciton (Scheme 1): (A) recombination within the nonfunctionalized regions of the SWCNT, leading to E_{11} photoluminescence; (B) trapping at a nondoped defect site, resulting in defect-activated, red-shifted E_{11}^- photoluminescence;[18,19] and (C) diffusion to an electron- or hole-doped defect site under highly reducing or oxidative conditions, generating E_T photoluminescence. E_T is further red-shifted than E_{11}^- due to the lowering of the trion energy by trapping in a defect-induced potential well.

Notably, trion photoluminescence is observed after covalent functionalization and subsequent processing in water and air, conditions that were previously expected to quench the required doping. This phenomenon persists even after the samples have been stored under ambient conditions for several months. We believe this doping longevity is due to the defect-induced trapping of the injected charge carriers. Such carrier trapping enables trions to form upon exciton diffusion to these doped defect sites.

It is important to note that the defects that we introduced to the nanotube sidewall are sp^3 centers in the sp^2 carbon lattice. Each sp^3 center is bonded to four atoms and is therefore perfectly satisfied from a valence perspective. The observed E_T photoluminescence occurs only when the functionalized structure is charged with electrons or holes. This situation is distinctly different from that of the atomic dopants used in semiconductors to produce donor-bound excitons, in which the donor electron is strongly correlated to the donor atom.[2] By analogy, a negative trion resembles a H^- ion, in which two electrons orbit a hole in place of a proton. It can be difficult to differentiate trions from donor-bound excitons, H_2 analogues in which the donor electron and the exciton electron are strongly correlated to their respective centers (the donor atom and the hole). These two extremes are the limiting cases of a more general theoretical

picture proposed by Rorison *et al.*[33] Although our experiments cannot rule out a H_2-like contribution, the H^- picture is expected to dominate. To allow the hole to be pinned at the radius of one electron such that it is not strongly correlated with the other electron, the effective mass of the hole has to be much larger than the effective mass of electron, as is the case with atoms. However, in SWCNTs, the effective mass of the hole is only slightly larger than the effective mass of the electron. Therefore, we attribute E_T to trions rather than donor-bound excitons.[34] Experiments that can observe the temperature-dependent evolution of trion populations may provide further evidence to support this picture.

CONCLUSIONS

We have demonstrated that controlled covalent defects in semiconducting carbon nanotubes promote generation of bound trions with the highest binding energy that has been reported (~260 meV). Efficient formation of this tricarrier quasi-particle in covalently modified, semiconducting SWCNTs is evident from the appearance of a new, bright photoluminescence peak that is substantially red-shifted from those of the parent excitons and trapped excitons. The strong defect dependence of these trions provides the opportunity to investigate the fundamental physics of these charged atomic analogues and to explore and control the chemistry and physics of SWCNT excited states through covalent modification. The ability to shift the excitation wavelength from the visible range to the near-IR can also be valuable for potential applications such as bioimaging, as interference from other materials in this wavelength range (1000−1400 nm) is minimized and the optical penetration depth of tissue can be maximized.[35,36]

METHODS

Chemical Routes to Bound Trions in Covalently Functionalized Carbon Nanotubes. All reagents were purchased from Sigma-Aldrich unless stated otherwise. Hexanoic acid functional groups were covalently attached to CoMoCat (6,5) SWCNT (SouthWest NanoTechnologies) sidewalls *via* propagative alkylcarboxylation using the Billups−Birch reduction.[20] This chemistry was repeated as desired to increase the degree of functionalization with each reaction cycle,[19] going as high as three cycles. CoMoCat (6,5) SWCNTs were dispersed with sodium (99%) in liquid ammonia (Airgas, 99.9%) condensed by an acetone/dry ice bath followed by the addition of 6-bromohexanoic acid (97%). Reaction cycles were completed by alternating the addition of sodium and 6-bromohexanoic acid. After evaporation of liquid ammonia, the sample was purified with nanopure water as per our previously published procedure[20] without aqueous extraction. (6,5) SWCNTs were also reduced using the Billups−Birch conditions, but without functionalization, by dispersing the starting material in liquid ammonia with sodium overnight. Functionalized or nonfunctionalized SWCNTs were dispersed in oleum for 4 h and washed with copious amounts of water until the filtrate pH returned to neutral.

4-Nitrobenzene-functionalized SWCNTs were synthesized using two different diazonium chemistries. The first reaction was an *in situ* method in which SWCNTs are individually dispersed in oleum (100%, 20% free SO_3) along with 4-nitroaniline (99+%), sodium nitrite (≥97%), and 2,2′-azobis(2-methylpropionitrile) (98%).[21] Functionalized samples were purified by quenching and washing with excess water and ethanol. After oven-drying, the sample was reduced by 0.75 or 1.5 molar equiv of sodium (with respect to moles of SWCNT carbon atoms) in liquid ammonia and purified the following day using the same procedure as was used for the purification of Billups−Birch alkylcarboxylated samples.

The second diazonium reaction employed 4-nitrobenzene diazonium salt, as previously reported.[18] CoMoCat (6,5) SWCNTs were individually dispersed in 1 wt % SDS−D_2O solution at a concentration of 30.2 mg/L. The SWCNTs were then functionalized by stirring the dispersed nanotubes with the freshly synthesized 4-nitrobenzene diazonium compound in a mole ratio of 300:1 (300 carbon atoms for every 1 molecule of diazonium salt) for 24 h in a light-shielded bottle to prevent degradation of the diazonium material. After 24 h, the solution was added to ethanol to remove surfactant, then filtered, washed, and dried at 80 °C overnight. A portion of the diazonium-functionalized (6,5) SWCNTs was redispersed in 1 wt % SDBS−D_2O. The remaining portion was reduced using the Billups−Birch conditions in approximately 35 mL of liquid ammonia. The reduced material was purified and subsequently redispersed in 1 wt % SDBS−D_2O for spectral analysis.

Spectroscopic Characterization of Bound Trions in Covalently Functionalized SWCNTs. For spectroscopic analysis, all samples were dispersed in 1 wt % SDBS (hard type, TCI-Japan)−D_2O (99.8% Cambridge Isotope Laboratories, Inc.) by probe-tip ultrasonication (Misonix) at an average power of 33 W for 2 h in a water-cooled, stainless-steel beaker, followed by ultracentrifugation with an Optima LE-80K Ultracentrifuge (Beckman Coulter) at 61 034*g* for 2 h to remove bundles. For the aqueous-phase diazonium chemistry, SWCNTs were dispersed in 1 wt % SDS−D_2O using the same procedure. D_2O is used as it has minimum absorption in the near-IR.

All surfactant-dispersed samples were diluted to an optical density of approximately 0.2 at the (6,5) E_{11} absorption peak and monitored with a Lambda 1050 UV−visible−NIR spectrometer (PerkinElmer) and a NanoLog spectrofluorometer (Horiba Jobin Yvon). The 970 nm excitation wavelength was produced using an external diode laser and a 1050 nm long-pass filter (Thorlabs). Loess smoothing was applied to the photoluminescence data. For Raman spectroscopy, surfactant was removed from the dispersed samples by immersion in ethanol, followed by drop-casting the flocculated material on a microscope slide. Raman scattering was measured on a LabRAM ARAMIS Raman microscope (Horiba Scientific) by averaging spectra from three different spots of the dried sample.

A van't Hoff plot was constructed from data obtained by monitoring the integrated peak area of the E_{11} and E_{11}^- photoluminescence of the Billups−Birch reacted CoMoCat (6,5) samples as the temperature was adjusted *via* water cooling under magnetic stirring. The cuvette temperature was ramped up and down between 10 and 90 °C, while the photoluminescence was monitored at discrete temperature points. The peak areas of the E_{11} and E_{11}^- emissions were fit using a Voigt area peak shape with PeakFit v4.12 software.

Conflict of Interest: The authors declare no competing financial interest.

Acknowledgment. We thank Charles W. Clark for helpful discussions on excitonic polarization. This research was supported in part by the University of Maryland, the Office of Naval Research (N000141110465), and the National Science Foundation (CAREER CHE-1055514). A.H.B. acknowledges the Department of Energy Office of Science Graduate Fellowship Program (DOE SCGF), made possible in part by the American Recovery and Reinvestment Act of 2009, administered by ORISE-ORAU

under Contract No. DE-AC05-06OR23100 for fellowship support.

Supporting Information Available: Excitation resonance photoluminescence emission, and UV−vis−NIR absorption spectra of Billups−Birch alkylcarboxylated SWCNTs, including after oleum treatment. Excitation−emission photoluminescence maps of 4-nitrobenzene diazonium-functionalized SWCNTs as well as photoluminescence emission spectra at different excitation wavelengths. Raman spectra of the 4-nitrobenzene diazonium-functionalized samples both before and after sodium reduction treatment. A van't Hoff plot of the Billups−Birch alkylcarboxylated SWCNTs. This material is available free of charge *via* the Internet at http://pubs.acs.org.

REFERENCES AND NOTES

1. Lampert, M. Mobile and Immobile Effective-Mass-Particle Complexes in Nonmetallic Solids. *Phys. Rev. Lett.* **1958**, *1*, 450–453.
2. Kheng, K.; Cox, R.; d'Aubigné, M.; Bassani, F.; Saminadayar, K.; Tatarenko, S. Observation of Negatively Charged Excitons X− in Semiconductor Quantum Wells. *Phys. Rev. Lett.* **1993**, *71*, 1752–1755.
3. Cox, R. T.; Huard, V.; Kheng, K.; Lovisa, S.; Miller, R. B.; Saminadayar, K.; Arnoult, A.; Cibert, J.; Tatarenko, S.; Potemski, M. Exciton Trions in II−VI Heterostructures. *Acta Phys. Pol.* **1998**, *94*, 99–109.
4. Warburton, R. J.; Dürr, C. S.; Karrai, K.; Kotthaus, J. P.; Medeiros-Ribeiro, G.; Petroff, P. M. Charged Excitons in Self-Assembled Semiconductor Quantum Dots. *Phys. Rev. Lett.* **1997**, *79*, 5282–5285.
5. Matsunaga, R.; Matsuda, K.; Kanemitsu, Y. Observation of Charged Excitons in Hole-Doped Carbon Nanotubes Using Photoluminescence and Absorption Spectroscopy. *Phys. Rev. Lett.* **2011**, *106*, 37404.
6. Park, J. S.; Hirana, Y.; Mouri, S.; Miyauchi, Y.; Nakashima, N.; Matsuda, K. Observation of Negative and Positive Trions in the Electrochemically Carrier-Doped Single-Walled Carbon Nanotubes. *J. Am. Chem. Soc.* **2012**, *134*, 14461–14466.
7. Santos, S.; Yuma, B.; Berciaud, S.; Shaver, J.; Gallart, M.; Gilliot, P.; Cognet, L.; Lounis, B. All-Optical Trion Generation in Single-Walled Carbon Nanotubes. *Phys. Rev. Lett.* **2011**, *107*, 1–5.
8. Mouri, S.; Miyauchi, Y.; Iwamura, M.; Matsuda, K. Temperature Dependence of Photoluminescence Spectra in Hole-Doped Single-Walled Carbon Nanotubes: Implications of Trion Localization. *Phys. Rev. B* **2013**, *87*, 045408.
9. Yuma, B.; Berciaud, S.; Besbas, J.; Shaver, J.; Santos, S.; Ghosh, S.; Weisman, R. B.; Cognet, L.; Gallart, M.; Ziegler, M.; *et al.* Biexciton, Single Carrier, and Trion Generation Dynamics in Single-Walled Carbon Nanotubes. *Phys. Rev. B* **2013**, *87*, 205412.
10. Rønnow, T. F.; Pedersen, T. G.; Cornean, H. D. Stability of Singlet and Triplet Trions in Carbon Nanotubes. *Phys. Lett. A* **2009**, *373*, 1478–1481.
11. Rønnow, T. F.; Pedersen, T. G.; Cornean, H. D. Correlation and Dimensional Effects of Trions in Carbon Nanotubes. *Phys. Rev. B* **2010**, *81*, 205446.
12. Wang, F.; Dukovic, G.; Brus, L. E.; Heinz, T. F. The Optical Resonances in Carbon Nanotubes Arise from Excitons. *Science* **2005**, *308*, 838–841.
13. Klingshirn, C. *Semiconductor Optics*, 2nd ed.; Springer: Berlin, 2005; pp 254−259.
14. Galland, C.; Imamoğlu, A. All-Optical Manipulation of Electron Spins in Carbon-Nanotube Quantum Dots. *Phys. Rev. Lett.* **2008**, *101*, 157404.
15. Wang, X.; Ren, X.; Kahen, K.; Hahn, M. A.; Rajeswaran, M.; Maccagnano-Zacher, S.; Silcox, J.; Cragg, G. E.; Efros, A. L.; Krauss, T. D. Non-blinking Semiconductor Nanocrystals. *Nature* **2009**, *459*, 686–689.
16. Bracker, A.; Stinaff, E. A.; Gammon, D.; Ware, M. E.; Tischler, J. G.; Park, D.; Gershoni, D.; Filinov, A. V.; Bonitz, M.; Peeters, F.; *et al.* Binding Energies of Positive and Negative Trions: From Quantum Wells to Quantum Dots. *Phys. Rev. B* **2005**, *72*, 035332.
17. Cognet, L.; Tsyboulski, D. A.; Rocha, J.-D. R.; Doyle, C. D.; Tour, J. M.; Weisman, R. B. Stepwise Quenching of Exciton Fluorescence in Carbon Nanotubes by Single-Molecule Reactions. *Science* **2007**, *316*, 1465–1468.
18. Piao, Y.; Meany, B.; Powell, L. R.; Valley, N.; Kwon, H.; Schatz, G. C.; Wang, Y. Brightening of Carbon Nanotube Photoluminescence through the Incorporation of sp^3 Defects. *Nat. Chem.* **2013**, *5*, 840–845.
19. Zhang, Y.; Valley, N.; Brozena, A. H.; Paio, Y.; Song, X.; Schatz, G. C.; Wang, Y. Propagative Sidewall Alkylcarboxylation That Induces Red-Shifted Near-IR Photoluminescence in Single-Walled Carbon Nanotubes. *J. Phys. Chem. Lett.* **2013**, *4*, 826–830.
20. Deng, S.; Zhang, Y.; Brozena, A. H.; Mayes, M. L.; Banerjee, P.; Chiou, W. A.; Rubloff, G. W.; Schatz, G. C.; Wang, Y. Confined Propagation of Covalent Chemical Reactions on Single-Walled Carbon Nanotubes. *Nat. Commun.* **2011**, *2*, 382.
21. Hudson, J. L.; Casavant, M. J.; Tour, J. M. Water-Soluble, Exfoliated, Nonroping Single-Wall Carbon Nanotubes. *J. Am. Chem. Soc.* **2004**, *126*, 11158–11159.
22. Avouris, P.; Freitag, M.; Perebeinos, V. Carbon-Nanotube Photonics and Optoelectronics. *Nat. Photonics* **2008**, *2*, 341–350.
23. Bachilo, S. M.; Balzano, L.; Herrera, J. E.; Pompeo, F.; Resasco, D. E.; Weisman, R. B. Narrow (*n*,*m*)-Distribution of Single-Walled Carbon Nanotubes Grown Using a Solid Supported Catalyst. *J. Am. Chem. Soc.* **2003**, *125*, 11186–11187.
24. Strano, M. S.; Huffman, C. B.; Moore, V. C.; O'Connell, M. J.; Haroz, E. H.; Hubbard, J.; Miller, M.; Rialon, K.; Kittrell, C.; Ramesh, S.; *et al.* Reversible, Band-Gap-Selective Protonation of Single-Walled Carbon Nanotubes in Solution. *J. Phys. Chem. B* **2003**, *107*, 6979–6985.
25. Ghosh, S.; Bachilo, S. M.; Simonette, R. A.; Beckingham, K. M.; Weisman, R. B. Oxygen Doping Modifies Near-Infrared Band Gaps in Fluorescent Single-Walled Carbon Nanotubes. *Science* **2011**, *330*, 1656–1659.
26. Kelly, K.; Sarkar, D.; Hale, G.; Oldenburg, S.; Halas, N. Threefold Electron Scattering on Graphite Observed with C60-Adsorbed STM Tips. *Science* **1996**, *273*, 1371–1373.
27. Spataru, C. D.; Ismail-Beigi, S.; Benedict, L. X.; Louie, S. G. Excitonic Effects and Optical Spectra of Single-Walled Carbon Nanotubes. *Phys. Rev. Lett.* **2004**, *92*, 077402.
28. Capaz, R. B.; Spataru, C. D.; Ismail-Beigi, S.; Louie, S. G. Diameter and Chirality Dependence of Exciton Properties in Carbon Nanotubes. *Phys. Rev. B* **2006**, *74*, 121401.
29. Mitroy, J.; Safronova, M. S.; Clark, C. W. Theory and Applications of Atomic and Ionic Polarizabilities. *J. Phys. B: At., Mol. Opt. Phys.* **2010**, *43*, 202001.
30. Shabrawy, K. El; Maharatna, K.; Bagnall, D.; Al-Hashimi, B. Modeling SWCNT Band-Gap and Effective Mass Variation Using a Monte Carlo Approach. *IEEE Trans. Nanotechnol.* **2010**, *9*, 184–193.
31. Lide, D. R., Ed. *CRC Handbook of Chemistry and Physics*, 82nd ed.; CRC Press: Boca Raton, FL, 2001.
32. Dacal, L. C. O.; Ferreira, R.; Bastard, G.; Brum, J. A. Binding Energy of Charged Excitons Bound to Interface Defects of Semiconductor Quantum Wells. *Phys. Rev. B* **2002**, *65*, 115325.
33. Rorison, J.; Herbert, D.; Dean, P.; Skolnick, M. A Model for the Neutral Donor Bound Exciton System in InP at High Magnetic Field. *J. Phys. C: Solid State Phys.* **1984**, *17*, 6435–6453.
34. Spataru, C. D.; Léonard, F. Quasiparticle and Exciton Renormalization Effects in Electrostatically Doped Semiconducting Carbon Nanotubes. *Chem. Phys.* **2013**, *413*, 81–88.
35. Chance, B. Near-Infrared Images Using Continuous, Phase-Modulated, and Pulsed Light with Quantitation of Blood and Blood Oxygenation. *Ann. N.Y. Acad. Sci.* **1998**, *838*, 29–45.
36. Welsher, K.; Sherlock, S. P.; Dai, H. Deep-Tissue Anatomical Imaging of Mice Using Carbon Nanotube Fluorophores in the Second Near-Infrared Window. *Proc. Natl. Acad. Sci. U.S.A.* **2011**, *108*, 8943–3948.